

Probabilistic Prediction of Neural Dynamics via Autoregressive Flow Matching

Nicole Rogalla¹, Yuzhen Qin¹, Mario Senden^{2, 3}, Ahmed El-Gazzar¹, and Marcel van Gerven¹

¹Department of Machine Learning and Neural Computing, Donders Institute for Brain, Cognition and Behaviour, Radboud University, Nijmegen, the Netherlands

²Department of Cognitive Neuroscience, Maastricht University, Maastricht, the Netherlands

³Maastricht Brain Imaging Center, Maastricht University, Maastricht, the Netherlands

Abstract: Forecasting neural activity in response to naturalistic stimuli remains a key challenge for understanding brain dynamics and enabling downstream neurotechnological applications. Here, we introduce a generative forecasting framework for modeling neural dynamics based on autoregressive flow matching (AFM). Building on recent advances in transport-based generative modeling, our approach probabilistically predicts neural responses at scale from multimodal sensory input. Specifically, we learn the conditional distribution of future neural activity given past neural dynamics and concurrent sensory input, explicitly modeling neural activity as a temporally evolving process in which future states depend on recent neural history. We evaluate our framework on the Algonauts project 2025 challenge functional magnetic resonance imaging dataset using subject-specific models. AFM significantly outperforms both a non-autoregressive flow-matching baseline and the official challenge general linear model baseline in predicting short-term parcel-wise blood oxygenation level-dependent (BOLD) activity, demonstrating improved generalization and widespread cortical prediction performance. Ablation analyses show that access to past BOLD dynamics is a dominant driver of performance, while autoregressive factorization yields consistent, modest gains under short-horizon, context-rich conditions. Together, these findings position autoregressive flow-based generative modeling as an effective approach for short-term probabilistic forecasting of neural dynamics with promising applications in closed-loop neurotechnology.

1 Introduction

Predicting how brain activity evolves over time in response to the environment is central to understanding neural systems and represents a key step toward closed-loop neurotechnology. Forecasting models provide a principled framework for investigating neural information processing, evaluating computational theories, serving as a key step toward closed-loop neurotechnology, where predicted neural activity informs adaptive, personalized interventions (Xiong et al., 2023). The challenge of forecasting neural dynamics is particularly pronounced in naturalistic settings, where complex, dynamic stimuli unfold over time, increasing predictive complexity while providing greater ecological validity (Zhou & Becker, 2025).

Across neural recording modalities, forecasting has emerged as a key focus to modeling neural dynamics (Antoniades et al., 2024; Chehab et al., 2022; Duan et al., 2025; Immer et al., 2025; W. Li et al., 2023; Lu et al., 2025; Lueckmann et al., 2025). In functional magnetic resonance imaging (fMRI), predictive approaches largely rely on encoding models that predict neural activity based on stimulus inputs (Naselaris et al., 2011), with examples including Eren et al. (2025), Güçlü and van Gerven (2015, 2017), Khosla et al. (2021), Scholz et al. (2025), and Yamins and DiCarlo (2016). The recent Algonauts project 2025 challenge further highlights the growing interest in predictive modeling under ecologically valid conditions by calling for the development of fMRI encoding models for multi-modal naturalistic stimuli (Gifford et al., 2025). Building on the challenge-winning encoding model TRIBE (d’Ascoli et al., 2025), recent work has extended this approach into a large-scale foundation model for in-silico neuroscience (d’Ascoli et al., 2026). Parallel advances in blood oxygenation level-dependent (BOLD) dynamics modeling have shown strong predictive performance in resting-state fMRI (Caro et al., 2024; Dvornek et al., 2019; Sobczak et al., 2021; Sun et al., 2024; Wein et al., 2022). Yet, few dynamics approaches extend to task-based fMRI modeling (Dorin et al., 2024; Paugam et al., 2024), with even fewer integrating both past stimuli and neural dynamics to forecast future BOLD responses, despite evidence of endogenous activity influencing stimulus processing (Arieli et al., 1996; Dehaghani & Zarei, 2025).

Despite these advances, most forecasting approaches remain deterministic, disregarding the intrinsic variability of neural dynamics and the noisy and indirect nature of fMRI recordings (Faisal et al., 2008; T. T. Liu, 2016; Tomko & Crapper, 1974). This limitation is particularly relevant in naturalistic experimental settings, where participants are exposed to continuous, high-dimensional real-world stimuli with increased complexity (Gifford et al., 2025; Gong et al., 2023; Simony & Chang, 2020; Y. Zhang et al., 2021). Generative models address this issue by yielding predictive distributions over possible future trajectories. This perspective resonates with the view that the brain itself may operate probabilistically: integrating noisy sensory inputs, internal states, and prior beliefs to generate behavior and perception aiming to reduce the prediction error (Millidge et al., 2022). Generative forecasting frameworks therefore not only improve

variability modeling but also provide a principled connection to theories of neural computation.

Probabilistic models of fMRI data have primarily been employed for decoding of external variables, such as movie ratings, from neural data, hemodynamic or connectivity modeling (Ajith & Calhoun, 2024; Alowadi et al., 2016; Battle et al., 2007; Friston et al., 2003; Harrison et al., 2015; J. Li & Tao, 2011; Safari & Mohammadbeigi, 2012; Svensen et al., 2000). Apart from recent exceptions such as a hierarchical diffusion model for fMRI forecasting introduced by Hu, Yujiang, et al. (2025), and the Brain Foundation Model (Bayazi et al., 2024), which builds on the success of large language models (LLMs), probabilistic models focusing on fMRI dynamics forecasting remain rare, leaving a clear methodological gap.

Beyond fMRI, probabilistic deep generative models have demonstrated strong performance in time series forecasting across diverse domains (Feng et al., 2024; Kolloviah et al., 2023; Meijer & Chen, 2024; Rasul et al., 2021). However, their computational costs have motivated the development of flow matching (FM) as a new training paradigm (Lipman et al., 2023). FM enables stable and efficient training by learning the transformation between simple base distribution and target distribution without the need for simulation. FM has recently been applied to time series forecasting (Hu, Wang, et al., 2025; Kolloviah et al., 2025; X. Zhang et al., 2025) with strong empirical results and fast training and sampling.

Existing FM methods, however, typically model the conditional distribution of the entire future trajectory, which poses a difficult optimization problem. To address this, El-Gazzar and van Gerven (2025a) proposed *autoregressive flow matching* (AFM), which decomposes forecasting into a sequence of one-step conditional distributions and requires autoregressively generating the next-step prediction during sampling. Their empirical results across classical dynamical systems and real-world data benchmarks show that AFM improves predictive accuracy compared to non-autoregressive FM baselines. This autoregressive formulation aligns the generative process with the temporal structure of the data. AFM is a natural fit for fMRI forecasting, as it unites the computational efficiency of flow-based generative models with the autoregressive modeling principles traditionally employed in fMRI modeling through Granger causality analyses and vector autoregressive models (Deshpande et al., 2009; Garg et al., 2011; Roebroek et al., 2005). By explicitly modeling temporal dependencies between successive states within the future segment, this approach further resonates with a dynamical systems perspective that interprets brain activity as an evolving process over time (Favela, 2021).

In this work, we introduce a large-scale generative framework for modeling neural dynamics using autoregressive flow matching that predicts parcel-wise BOLD activity in the short-term future. By learning the conditional distribution of future neural activity given both past BOLD dynamics and naturalistic sensory input, our model moves beyond stimulus-only and deterministic approaches, enabling uncertainty-aware predictions and realistic generative sampling of neural trajectories. This framework combines the neurosci-

entific appeal of autoregressive modeling with the stability and efficiency of modern flow-based generative methods. Using the large-scale Algonauts project 2025 challenge fMRI dataset, we demonstrate predictive performance and uncertainty quantification of neural activity at scale. AFM significantly outperforms both the official challenge general linear model baseline and a non-autoregressive FM baseline in forecasting multi-step short-term parcel-wise BOLD activity, yielding consistently higher noise-ceiling-adjusted correlations across subjects and cortical regions. These results indicate that AFM approaches the performance noise ceiling imposed by the measurement modality, which is the maximum predictable variance given measurement noise and intrinsic neural variability, bringing neural forecasting closer to the accuracy required for downstream applications.

2 Methods

2.1 Dataset

This study utilizes datasets from the Courtois Project on Neural Data Modeling (NeuroMod, <https://www.cneuromod.ca/>) *friends* and *movie10* as provided by the Algonauts project 2025 challenge "How the Human Brain Makes Sense of Multimodal Movies" (Boyle et al., 2023; Gifford et al., 2025). It contains single-subject BOLD response recordings to naturalistic stimuli for four subjects. fMRI BOLD responses were recorded using a 3T Siemens Prisma Fit scanner with a repetition time (TR) of 1.49s. Responses were normalized to the Montreal Neurological Institute (MNI) spatial template and averaged to 1000 functionally defined brain parcels (Schaefer et al., 2017). The *friends* dataset encompasses seasons 1 to 6 of the Sitcom *Friends*. The *movie10* dataset consists of three feature movies (*Bourne Supremacy*, *The Wolf of Wall Street*, *Hidden Figures*) and a documentary (*Life documentary*), with *Hidden Figures* and *Life* having been watched twice. The dataset encompassed approximately 65 hours (55 hours of *friends* and 10 hours of *movie10*) of movie stimuli content. Stimuli were presented in English and are available as movie frames, audio samples and language transcripts. For more detailed information on the fMRI dataset, please consult the Courtois NeuroMod's Project documentation (<https://docs.cneuromod.ca/>).

2.2 Relation to the Algonauts project 2025 challenge

The Algonauts project 2025 challenge focuses on stimulus-only encoding models and explicitly prohibits the use of past BOLD dynamics as inputs to the prediction model. The phase 1 leaderboard evaluates

predictions for *Friends* season 7, whose BOLD responses have not been publicly released. Our approach explicitly utilizes past BOLD dynamics to model temporal dependencies. As a result, our framework cannot be applied to the official season 7 test set and we instead evaluate forecasting performance on season 6. Our results are therefore not directly comparable to the challenge leaderboard due to differences in training and test set, model input (stimulus and BOLD dynamics vs. stimulus-only) and difference in prediction horizon, given that we perform multi-step forecasting while challenge models are focused on one-step prediction. We report the official general linear model (GLM) baseline as a classical encoding model reference that anchor our results within the challenge context. Retraining winning challenge models under our settings was not pursued due to the substantial computational demands of the top-performing approach (d’Ascoli et al., 2025).

2.3 Stimulus features

Stimulus features were extracted using the Algonauts project 2025 challenge development kit (Gifford et al., 2025), comprising visual, auditory and linguistic embeddings from pretrained models. Visual features were extracted using a Slow R50 (Feichtenhofer et al., 2019) pretrained on Kinetics 400 (Kay et al., 2017), capturing spatiotemporal action information. Auditory features were mel-frequency cepstral coefficients representing human frequency perception (Abdul & Al-Talabani, 2022). Linguistic features were obtained from the large language model *Bidirectional Encoder Representations from Transformers* (BERT) (Devlin et al., 2019), providing contextual word embeddings from the episode transcripts. More details on feature extraction can be found in Supplementary Section S1.

2.4 Flow-matching-based generative modeling

Before describing our autoregressive flow matching framework, we briefly outline the principles of flow-based generative modeling that underpin our approach. Generative models aim to learn a mapping from a simple base distribution p^0 to a complex data distribution p^1 (Ruthotto & Haber, 2021). This transformation can be defined through a continuous normalizing flow (CNF) as a solution to an ordinary differential equation (ODE) (Chen et al., 2019). This flow $\psi: \Omega \times [0, 1] \rightarrow \Omega$ on data space Ω evolves a sample $x^0 \sim p^0$ into a target sample $x^1 := \psi(x^0, 1) \sim p^1$ by solving the initial value problem

$$d\psi(x, s) = \mu(\psi(x, s), s) ds, \quad \psi(x, 0) = x_0, \quad s \in [0, 1]. \quad (1)$$

The vector field $\mu: \Omega \times [0, 1] \rightarrow \Omega$, that defines the velocity of the flow and generates the probability path $(p^s)^{0 \leq s \leq 1}$, is to be learned.

Conditional flow matching (Lipman et al., 2023) is a simulation-free training method of CNFs that avoids numerically solving ODEs during training. Instead, it learns a neural vector field v_θ with trainable parameters θ to approximate the intractable target vector field μ by regressing against per-example conditional optimal vector fields $\mu(x, s|z)$ conditioned on an arbitrary random variable z with probability density function p_z :

$$\mathcal{L}_{\text{CFM}}(\theta) = \mathbb{E}_{s \sim U(0,1), z \sim p_z, x \sim p^s(x|z)} \|\mu(x, s|z) - v_\theta(x, s)\|^2. \quad (2)$$

This framework allows efficient and stable training of generative models and provides the basis for our autoregressive flow matching extension.

2.5 Autoregressive flow matching

Problem setting Let $y_\tau \in \mathbb{R}^n$ denote the fMRI BOLD response of n brain parcels at time τ . Given access to l past fMRI images including the current image, denoted as $Y_l = \{y_{\tau-l}, \dots, y_\tau\}$, the objective is to predict the next f future images $Y_f = \{y_{\tau+1}, \dots, y_{\tau+f}\}$, conditioned on both past images and stimulus feature input $C = \{C_l, C_f\}$ with past stimulus features $C_l = \{c_{\tau-l}, \dots, c_\tau\}$ and future stimulus features $C_f = \{c_{\tau+1}, \dots, c_{\tau+f}\}$. Formally, the goal is to learn a conditional distribution $p(Y_f | Y_l, C)$ from a dataset $\mathcal{D} = \{(Y_f^i, Y_l^i, C^i)\}_{i=1}^m$ composed of m training sequences. Once learned, this distribution can be sampled to generate future BOLD trajectories conditioned on observed history and stimulus features.

Training approach AFM introduced by El-Gazzar and van Gerven (2025a) is the backbone of our generative modeling framework. BOLD time series forecasting is treated as sampling from a learned conditional distribution of future BOLD images given historical images and stimulus features. Unlike standard flow matching, which predicts the all f future BOLD images jointly, this approach decomposes the forecasting task into sequential next-image predictions. The conditional distribution can be factorized autoregressively:

$$p(Y_f | Y_l, C) = \prod_{t=\tau+1}^{\tau+f} p(y_t | y_{t-w:t-1}, c_{t-w:t}) \quad (3)$$

with temporal context window $w \leq l$.

From base distribution $p^0(y_t) = \mathcal{N}(0, I)$ to data distribution $p^1(y_t)$, the conditional probability path is defined as $p^s(y_t | z) = \mathcal{N}((1-s)y_t^0 + sy_t^1, \sigma^2 I)$ using an ODE with conditional optimal vector field

$\mu(y_t, s | z) = y_t^1 - y_t^0$ with $z = \{y_t^0, y_t^1\}$, $y_t^0 \sim p^0$ and $y_t^1 \sim p^1$.

The neural velocity field ν_θ is learned by regressing against the target velocity field μ given the following training objective

$$\mathcal{L}(\theta, \phi) = \mathbb{E}_{z \sim \pi_{0,1}, s \sim \mathcal{U}(0,1), y_t^s \sim p^s(y_t | z)} \|\mu(y_t^s, s | z) - \nu_\theta(y_t^s, h_t, c_t, s)\|^2 \quad (4)$$

with $h_t = \zeta_\phi(y_{t-w:t-1}, c_{t-w:t-1})$ being the context encoding with encoder ζ_ϕ . $\pi_{0,1}$ denotes a data coupling over pairs (y_t^0, y_t^1) , where $y_t^0 \sim p^0$ and $y_t^1 \sim p^1$. Sampling requires solving the ODE. At inference, forecasts are generated in an autoregressive manner by iteratively sampling from each conditional distribution using the learned flow. Figure 1 depicts a visual representation of this framework.

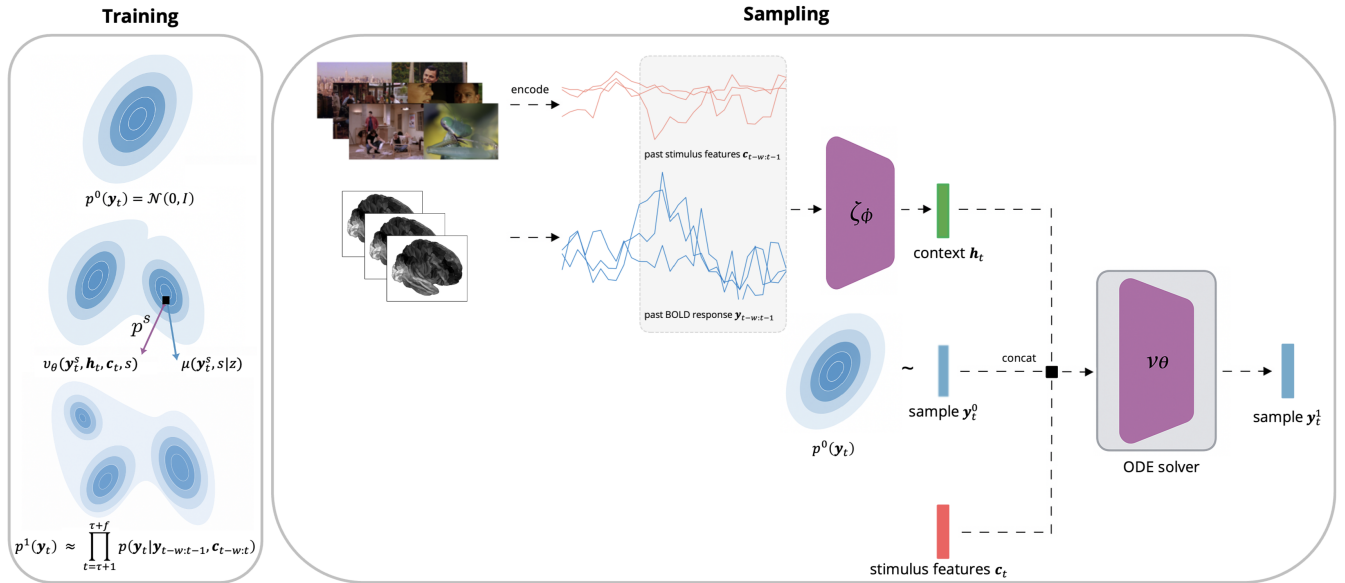


Figure 1: Autoregressive flow matching framework. Training aims to construct a probability path between a base distribution p^0 and the target distribution p^1 . The path is learned by regressing a neural network ν_θ which processes a sample from the probability path y_t^s at flow step s , a context vector h_t encoding both past BOLD images and stimulus features in a context window of length w , the stimulus feature c_t , against the target conditional velocity field μ . Predictions are generated by sampling from p^0 and integrating ν_θ with an ODE solver until $s = 1$. Figure adapted from El-Gazzar and van Gerven (2025a).

Implementation details Our model consists of: (i) an encoder ζ_ϕ (gated recurrent units, GRU) that maps multimodal features into latent states, (ii) a neural dynamics model ν_θ (time-conditioned dense layers) that evolves latent trajectories using 16-dimensional Fourier positional embeddings to encode the flow step s , and (iii) a decoder λ_θ (linear layer) mapping latents to predicted BOLD. An overview of selected hyperparameters can be found in Supplementary Table S6, details on tuning are supplied in Supplementary Section S3.4. For an evaluation of alternative encoders see Supplementary Section S3.3.

Training details Training was performed on a single NVIDIA A100 GPU using the Adam optimizer. Each model was trained with mean squared error loss for up to 20,000 steps, with early stopping after 1,000 training steps on a 10% validation split. The temporal context window is 30s (22 TRs). One model was trained per subject (for comparisons with group-level models see Supplementary Section S3.5).

2.6 Baselines

As a reference to the Algonauts project 2025 challenge, we include the official general linear model (GLM) provided with the challenge toolkit with slight modifications as a baseline. Notably, this model is a simple stimulus-to-BOLD encoding approach that functions merely as a connection to the challenge and a lower-bound on performance rather than serving as a competitive baseline. Our main comparison is to a non-autoregressive standard flow matching (SFM) that utilizes the same historical inputs as AFM but predicts future BOLD activity segments jointly (for more information see Supplementary Section S2).

2.7 Performance evaluation

Performance was evaluated on the held-out *Friends* season 6 test set of the Algonauts project 2025 challenge dataset. Predictions were averaged over 100 independent samples obtained by autoregressively sampling from the learned conditional distribution by solving the ODE with Euler’s method with $dt = 0.01$ using a rolling-window approach within the $f = 10s$ (8 TRs) prediction horizon and concatenating these segments to yield full predictions. This avoids accumulation errors during inference. The first and last five samples of each episode were removed in line with the Algonauts project 2025 challenge scoring.

Performance was quantified using Pearson correlation r between predicted and observed BOLD, averaged across parcels, subjects, and groups, with noise-ceiling adjustment (see Supplementary Section S4). Significance against chance-level and of model comparisons was assessed using block permutation tests (Adolf et al., 2014), with 30s block length, random circular shift, 10,000 repetitions and deemed statistically significant at $p < 0.05$. At the parcel level, multiple comparisons were corrected using the False Discovery Rate (FDR) procedure of Benjamini–Hochberg, while above the parcel level, Bonferroni correction was applied.

2.8 Uncertainty quantification

Uncertainty was evaluated using the continuous ranked probability score (CRPS), which quantifies how well the predictive distribution aligns with the observed BOLD response. For each framework, the CRPS was computed at every time step and then averaged over the full predicted time series.

2.9 Temporal and spatial analyses

We conducted network-level analysis based on the seven large-scale networks defined by Yeo et al. (2011) (see Supplementary Figure S7), and ablations varying context window length within the range of 0-50s and prediction horizon within the range of 0-25s.

3 Results

3.1 AFM significantly outperforms baselines

AFM significantly outperforms both GLM and non-autoregressive flow matching in forecasting future neural dynamics across all subjects (see Table 1 and Supplementary Table S7). To contextualize predictive performance, we estimated noise ceilings, providing an upper bound on predictable variance given measurement noise and intrinsic variability. Across subjects, the noise ceilings are relatively low (mean $r = 0.588$; see Supplementary Table S8), reflecting the inherent difficulty of predicting BOLD dynamics. AFM improves mean test performance by 79% compared to GLM-based challenge baseline ($r_{AFM}^* = 0.465$ vs. $r_{GLM}^* = 0.260$) and by 11% compared to SFM ($r_{AFM}^* = 0.465$ vs. $r_{SFM}^* = 0.420$). Although SFM attains higher train r^* , its larger train–test gap suggests overfitting, whereas AFM yields better generalization and earlier convergence (see Supplementary Figure S5). This demonstrates that FM is a competitive approach for predicting BOLD dynamics, and that incorporating autoregressive modeling yields clear benefits.

AFM’s advantage was consistent across several encoder architectures (see Supplementary Section S3.3). LSTM and GRU performed best, while simpler sRNNs lagged. GRU was used for all subsequent analyses due to comparable accuracy and faster training. We also compared group-level and individual AFM models; results (see Supplementary Section S3.5) show that subject-specific models consistently outperform pooled models, consistent with prior findings on inter-individual variability in fMRI responses.

Table 1: Performance comparison of AFM to baselines (SFM and GLM). Noise-ceiling adjusted Pearson's correlation scores (r^*) per subject for GLM baseline and FM optimized individual models. Train correlations are based on season 1, test correlations are based on season 6 of the TV show *Friends*. Values are rounded to three decimals. Highest values per column are highlighted in bold. All comparisons between frameworks significant given block-permutation test (10,000 repetitions, $p < 0.05$).

Framework	Train r^*					Test r^*				
	mean	sub-01	sub-02	sub-03	sub-05	mean	sub-01	sub-02	sub-03	sub-05
GLM (Algonauts project 2025 challenge baseline)	0.320	0.330	0.331	0.312	0.309	0.260	0.242	0.275	0.267	0.256
SFM	0.577	0.597	0.546	0.584	0.606	0.423	0.402	0.405	0.447	0.438
AFM	0.498	0.480	0.437	0.541	0.532	0.465	0.449	0.428	0.493	0.488

3.2 AFM achieves widespread spatial prediction performance gains

Across subjects, AFM achieved widespread positive correlations throughout the cortex, with mean raw correlation scores (mean: 0.273; sub-01: 0.276; sub-02: 0.246; sub-03: 0.303; sub-05: 0.269; see Fig. 2A), with on average all parcels significantly predicted (block-permutation test; 10,000 repetitions; $p < 0.05$; FDR correction). Spatial patterns were highly consistent across individuals, with variability largely in the magnitude rather than the location of peak correlations. The spatial distribution of prediction performance was qualitatively similar to patterns of average activity and noise ceilings, with higher correlations in parcels exhibiting greater activity and higher noise ceilings (see Supplementary Figure S8).

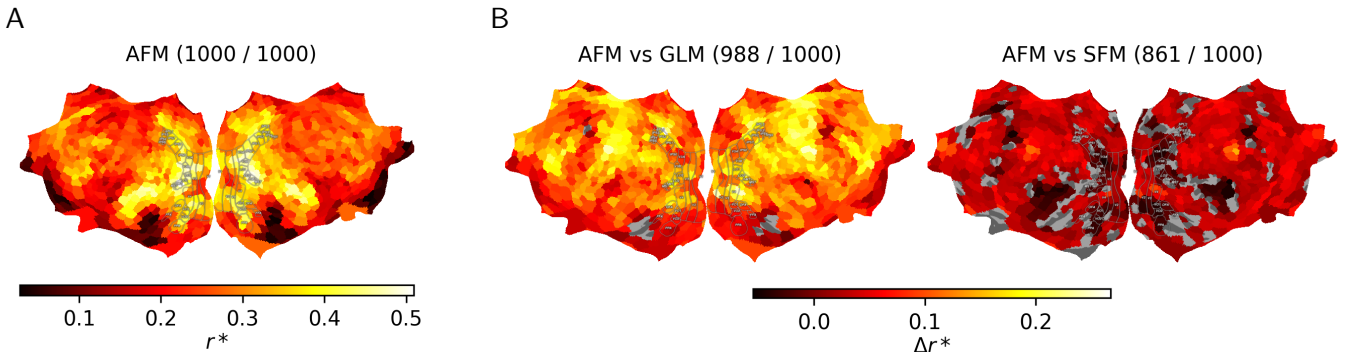


Figure 2: Flatmap of mean prediction performance of AFM. A) Flatmap of parcel-wise Pearson's correlation coefficients (r) between predicted and observed fMRI responses averaged across subjects displayed on the FreeSurfer fsaverage brain. B) Flatmap of parcel-wise performance difference between (1) GLM and AFM and (2) SFM and AFM. Errorbar shared for difference plots. Insignificant parcels are depicted in grey (block-permutation test; 10,000 repetitions; $p < 0.05$, FDR-corrected across parcels). Numbers in parentheses indicate the count of significant parcels out of the total 1,000.

Relative to GLM, AFM increased both the number of significant parcels (1000 vs 998) and the mean correlation (mean $\Delta r^* = +0.119$; see Supplementary Figure S10A). Performance difference is significant for on average 988 parcels with mean gains of $\Delta r^* = +0.120$ (see Figure 2B). Compared to SFM,

AFM gains are less pronounced. Regardless, AFM outperforms mean r^* (mean $\Delta r^* = +0.023$; see Supplementary Figure S10B). While AFM yields broader whole-brain performance, SFM exhibits higher maximum r in few occipital and temporal parcels, indicating more localized peaks. Performance difference is significant for on average 861 parcels with mean gains of $\Delta r^* = +0.024$ (see Figure 2B). For a detailed overview of spatial performance per subject see Supplementary Figures in Section S5.4.

3.3 AFM results in gains across large-scale cortical networks

AFM improves performance over both baselines across all seven large-scale cortical networks as specified by Yeo et al. (2011) (see Figure 3 and Supplementary Figure S7 for a flatmap of the networks). Performance is lowest in the limbic network, consistent with its comparatively low noise ceiling (see Supplementary Table S9). Gains over GLM are largest in somatomotor (+0.144) and frontoparietal (+0.133) networks and notably smallest for the limbic network (+0.040); gains over SFM are smaller but consistently positive (+0.021 to +0.036). All improvements are significant, except for gains compared to SFM in the visual network ($r_{\text{diff}}^* = 0.006$, $p^* = 1.0$).

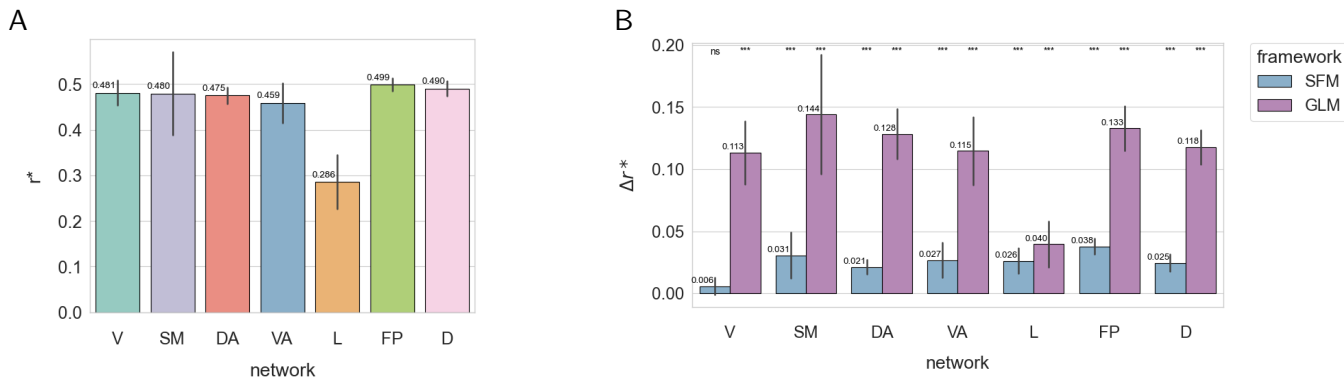


Figure 3: Prediction performance of optimized individual AFM models with GRU encoder across Yeo et al. (2011)'s seven brain networks. A) Noise-level-adjusted correlation test scores (r^*) averaged over parcels within each network. Error bars indicate variability across subjects. All results significant (block-permutation test, 10,000 repetitions, $p < 0.001$, Bonferroni correction). B) Relative performance gains ($\Delta r = r_{\text{AFM}}^* - r_B^*$) of AFM over baseline frameworks (GLM, SFM). Asterisks denote significance levels of differences given a block-permutation test (10,000 repetitions, *: $p < 0.05$, **: $p < 0.001$, ***: $p < 0.001$, ****: $p < 0.0001$, ns: not significant; Bonferroni correction). Abbreviations: V: visual, SM: somatomotor, DA: dorsal attention, SV: salience / ventral attention, L: limbic, FP: frontoparietal, D: default. Results rounded to three decimals.

3.4 AFM shows comparable uncertainty quantification to SFM

Across all subjects, AFM yields marginally improved uncertainty quantification compared to the baseline SFM. As shown in Table 2, AFM achieved a lower CRPS both on average (0.369 vs. 0.370) and consistently across individual subjects, although the differences are small. For visual inspection of confidence intervals see Supplementary Figure S6.

Table 2: Uncertainty quantification of AFM compared to baseline SFM. Continuous ranked probability score (CRPS) per framework on test set predictions. Values are rounded to three decimals. Best values per column are highlighted in bold.

	CRPS				
	mean	sub-01	sub-02	sub-03	sub-05
SFM	0.370	0.368	0.361	0.378	0.374
AFM	0.369	0.366	0.359	0.377	0.373

3.5 Ablation study: AFM benefits from longer context windows and shorter prediction horizons

We evaluated the performance of both probabilistic frameworks given different context and prediction windows on subject 1. Increasing the context window length improved performance for both frameworks, with the effect being substantially stronger for AFM. While SFM showed only modest gains across the tested range, AFM exhibited a steady rise in r^* , with performance diverging from SFM once the context exceeded roughly 15s (see Figure 4A).

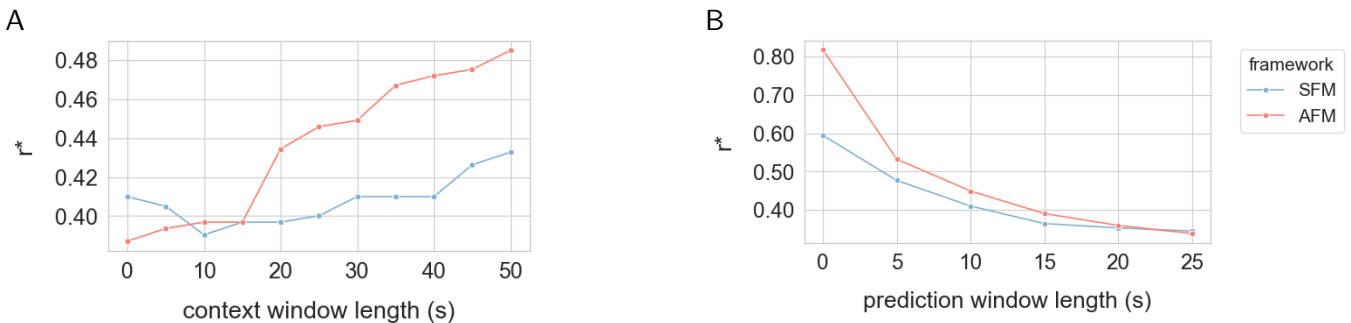


Figure 4: Ablation analyses of A) context window length and B) prediction window length for AFM and SFM on subject 1. Noise-ceiling adjusted correlation (r^*) shown for frameworks evaluated in increments of 5 (0-50s for context: 0-25 s for prediction). Markers indicate observed values.

In contrast, with increased prediction window length, r^* decreased for both frameworks. The decline is steeper for AFM, though AFM achieves higher r^* than SFM across most window lengths, with the

largest advantage at short horizons. At the longest prediction window ($s = 25$), AFM’s performance is slightly below that of SFM (see Figure 4B).

3.6 Ablation study: Past BOLD dynamics are critical for predictive performance

To isolate the contribution of past neural dynamics, we compared FM models trained with both past BOLD and stimulus features to FM models trained on only stimulus history. Removing past BOLD context resulted in a substantial reduction in predictive performance compared to the full model (AFM: mean $r^* = 0.465$ vs $r^* = 0.284$, SFM: mean $r^* = 0.423$ vs $r^* = 0.162$; Table 3). This performance drop was consistent across all subjects and reduced the model to a level only marginally above the stimulus-only official GLM baseline.

Table 3: Performance of FM models trained using both past stimulus and BOLD dynamics compared to FM models given only stimulus history. Noise-ceiling adjusted Pearson’s correlation scores (r^*) per subject. Test correlations are based on season 6 of the TV show *Friends*. Values are rounded to three decimals.

	mean	sub-01	sub-02	sub-03	sub-05
AFM (BOLD + stimulus)	0.465	0.449	0.428	0.493	0.488
AFM (stimulus only)	0.284	0.274	0.284	0.298	0.279
SFM (BOLD + stimulus)	0.423	0.402	0.405	0.447	0.438
SFM (stimulus only)	0.162	0.165	0.161	0.181	0.141

4 Discussion

In this work, we introduced a probabilistic forecasting framework for neural dynamics based on autoregressive flow matching that produces short-term BOLD time series predictions. Using the large-scale naturalistic fMRI Algonauts project 2025 challenge dataset, we show that AFM improves predictive performance over the challenge baseline and non-autoregressive standard flow matching. Across subjects, AFM consistently achieves the highest predictive correlations, and, in comparison to SFM, reduces overfitting, with spatial and network-level analyses confirming widespread improvements across the cortex. Our findings extend prior demonstrations of AFM’s performance (El-Gazzar & van Gerven, 2025a) to the biologically noisy and high-dimensional regime of fMRI. Our results position AFM as a promising framework for forecasting neural dynamics in naturalistic settings, as it aligns with both the temporal and stochastic properties of brain activity.

The strong performance of our probabilistic forecasting framework is largely driven by its explicit use of historical BOLD dynamics, which reflect contributions of ongoing brain dynamics, including endogenous activity, that shape future neural responses (Arieli et al., 1996; Dehaghani & Zarei, 2025). While previous approaches to predicting future neural activity focus on encoding models, which disregard past activity, we demonstrate that utilizing past BOLD dynamics improves forecasting performance. Internal ablations show that conditioning only on stimulus features causes a sharp performance drop for both FM variants. In this stimulus-only setting, AFM effectively collapses to a one-step-ahead encoder model, achieving performance only marginally above the GLM baseline. This pattern suggests that the primary source of performance gains in both FM models arises from conditioning on past BOLD dynamics rather than requiring increased architectural complexity, as in recent challenge-winning encoding models (d’Ascoli et al., 2025; Schad et al., 2025), which demand substantially greater computational resources. Relating our findings to the Algonauts project 2025 challenge, we not only outperform the lower-bound reference of the simple official challenge GLM baseline encoding model, but also the more competitive contextual benchmark of the one-step ahead cluster-based multi-layer perceptron encoding model (Corsico et al., 2025), which is, to the best of our knowledge, the only model reporting results for season 6 with a noise-ceiling adjusted score of $r^* = 0.453$. Under a comparable one-step ahead forecasting setting ablations of both our flow-matching models exceed this level ($r^* = 0.595$ for SFM; $r^* = 0.818$ for AFM), and AFM remains competitive even in our more challenging multi-step setting ($r^* = 0.465$). A direct comparison to the full Algonauts project 2025 challenge leaderboard is not possible due to differing test sets and training regimes. Under comparable one-step-ahead settings in our setup, history-aware models outperform stimulus-only variants, suggesting that excluding past neural state can be a limiting assumption for neural dynamics forecasting. This finding aligns with evidence that prestimulus and ongoing activity shapes sensory processing and perception (Arieli et al., 1996; Dehaghani & Zarei, 2025) and motivates a shift from static stimulus–response mappings toward history-aware models.

While conditioning on past neural activity accounts for the most prominent performance gains compared to one-step ahead encoding models, our focus lies on multi-step forecasting motivated by downstream use-cases within closed-loop neurotechnology. Aligning with a dynamical systems perspective on neuroscience (El-Gazzar & van Gerven, 2025b), we explicitly model the temporal structure through the autoregressive formulation of AFM. This yields statistically significant and modest improvements in short-term forecasting of BOLD dynamics compared to SFM. Across subjects, AFM outperformed SFM throughout the majority of parcels and across most major large-scale functional networks, demonstrating that autoregressive factorization provides a systematic advantage under short-horizon, context-rich conditions, that is especially valuable for naturalistic settings which engage distributed brain systems (Sonkusare et al., 2019). While SFM models the future trajectory jointly and does not explicitly enforce dependen-

cies between successive future states, AFM factorizes prediction into sequential one-step conditionals, enforcing temporal continuity by autoregressive sampling in the generative process. This distinction has different implications across cortical networks. In strongly stimulus-driven regions such as the visual network (Ito et al., 2020), temporal structure is largely imposed by the stimulus itself through tight stimulus–response locking. One interpretation is that SFM can implicitly recover temporal dependencies from stimulus features alone, yielding performance comparable to AFM. In contrast, in networks whose activity is less stimulus-driven and temporally extended, such as the default and frontoparietal systems, temporal dependencies are less coupled to the stimulus (Ito et al., 2020). Here, explicitly enforcing temporal structure through autoregressive factorization provides a meaningful inductive bias, leading to improved forecasting performance.

Temporal ablations on subject 1 further suggest that increasing temporal context led to clear performance improvements for AFM across networks, whereas SFM showed only weak sensitivity to additional context. This pattern suggests that AFM is better able to translate extended history into constraints on the evolution of future activity, whereas for SFM enlarging the context window primarily increases the dimensionality of the conditioning space. AFM’s context-related gains were smallest in visual cortex and larger in association networks, a pattern potentially related to previously reported hierarchical differences in intrinsic processing timescales (Ito et al., 2020; Murray et al., 2014; Raut et al., 2020), although these results are not fully consistent due to higher gains in the somatomotor network. However given that these analyses are limited to a single subject, the results should be interpreted cautiously and warrant further investigation (see Supplementary Figures S14 and S15).

Moreover, by learning a simpler conditional distribution, AFM converges more rapidly during training and exhibits reduced overfitting relative to SFM. This suggests that autoregressive factorization not only improves predictive accuracy but also facilitates more stable and efficient learning, an important consideration for large-scale neural forecasting models.

Together, these analyses support the view that autoregressive formulations more effectively capture temporal dependencies in BOLD dynamics and improve forecasting performance, in line with prior work on autoregressive modeling of neural time series (Deshpande et al., 2009; Garg et al., 2011; Rogers et al., 2010; Seth, 2010; Sobczak et al., 2021). Importantly, these gains are primarily observed in short-horizon, context-rich settings, a limitation we discuss in detail below.

Beyond predictive performance, a key strength of generative modeling for naturalistic fMRI, is their ability to quantify predictive uncertainty arising from neural variability and measurement noise as evidenced by the low noise ceiling (see Supplementary Table S8) which highlights the inherent difficulty of predicting accurately. Such uncertainty estimates are crucial for risk-aware decision-making in prospective clinical

settings, but also for evaluating how well a model captures the underlying neural dynamics. The slightly improved predictive distributions generated by AFM compared to SFM, which are consistently lower across subjects, networks and a majority of parcels (see Supplementary Figures S12 and S13), suggest that aligning the generative process with explicit temporal structure may be associated with small improvements in uncertainty calibration. Detailed statistical analyses will be needed to fully quantify this effect. Such improvements are particularly relevant given that well-calibrated predictive uncertainty is foundational for reliable model-based control and closed-loop neurotechnologies.

While these results position AFM as a promising approach for short-term probabilistic forecasting of neural dynamics, they should be interpreted in light of several limitations that also point toward directions for future work. First, model optimization was constrained by computational resources, limiting the breadth of the search space and necessitating tuning on group-level rather than on individual models. This constraint also led us to rely on the PCA-reduced multimodal stimulus features provided by the Algonauts project 2025 challenge. However, substantial performance improvements may be achievable with more expressive features, such as those used by the challenge winner (d'Ascoli et al., 2025). Moreover, the performance variability we observe across encoder types within our own framework (see Supplementary Section S3.3) suggests that further exploration of encoder architectures could yield significant additional gains. Second, our comparison focused on each frameworks' best-performing configuration instead of a parameter-matched evaluation, which may bias the performance comparison between AFM and SFM. Third, the sequential sampling procedure required by AFM introduces higher inference latency. This creates a trade-off between predictive accuracy and computational speed that is particularly relevant for real-time or online applications. Fourth, temporal ablations in subject 1 suggest that AFM's advantage is largely confined to short-term forecasting and to settings with sufficiently rich temporal context. At longer prediction horizons, performance degrades more drastically than for SFM, consistent with error accumulation in autoregressive models. At shorter context windows, AFM's performance is lower than SFM's, as the latter's joint modeling can mitigate the impact of limited contextual information.

Future research should focus on the robustness and generalizability of our findings by evaluating out-of-distribution performance across stimulus types, scanners, and demographic groups (Rohlf's, 2025). Establishing such generalization is essential before deploying these models in downstream settings. Building on this foundation, AFM's ability to generate short-horizon, uncertainty-aware neural forecasts positions it as a promising component for emerging neurotechnological applications. Its subject-specific multi-step ahead formulation makes it particularly attractive for integration into model-predictive neural control frameworks (Schwenzer et al., 2021), supporting personalized closed-loop interventions for conditions such as epileptic seizures (Chakravarthy et al., 2009; Z. Liu et al., 2025), and informing adaptive neurostimulation strategies (Carè et al., 2024). Realizing such downstream applications will require a high

level of predictive accuracy. While the prediction performance of AFM models indicates that a substantial fraction of the explainable signal is captured, the relatively low noise ceilings of this dataset (see Supplementary Table S8) reflect the inherent difficulty of predicting BOLD dynamics. Consequently, even a model reaching this limit would not necessarily guarantee that the resulting forecasts are sufficient for all downstream applications, as the noisy, indirect and temporally delayed nature of the BOLD signal imposes additional challenges on neural interventions. Achieving performance suitable for such applications will therefore potentially require both richer neural measurements, such as data with a higher temporal resolution or reduced noise, and further advances in model capacity, for example through more expressive encoders or modality-informed decoders. Finally, future methodological advances could focus on moving from the discrete-time formulation used herein toward continuous-time approaches that more faithfully capture the dynamical nature of brain activity. In particular, stochastic neural differential equations (Kidger, 2022) offer a promising direction for modeling both the temporal continuity and inherent stochasticity of neural systems and can serve as a powerful basis for white-box forecasting models (El-Gazzar & van Gerven, 2024).

5 Conclusion

In this work, we introduced a probabilistic, history-aware framework for forecasting neural dynamics based on autoregressive flow matching and evaluated it in a large-scale naturalistic fMRI setting. Our results show that incorporating past BOLD dynamics is a key driver of forecasting performance, substantially outperforming stimulus-only encoding approaches. Beyond this dominant effect, we find that autoregressive factorization yields consistent improvements in short-horizon forecasting relative to non-autoregressive flow matching. By enabling distributional predictions of future neural activity, our approach is suited to capture neural variability and measurement noise while further supports uncertainty-aware modeling of BOLD dynamics, a prerequisite for reliable downstream use. While important challenges remain, our work provides a foundation for future advances in forecasting-based modeling of neural dynamics that explicitly incorporates temporal dynamics and uncertainty.

6 Ethics

This work uses the CNeuroMod dataset provided through the Algonauts project 2025 challenge. All participants provided informed consent for data collection and sharing. The dataset is publicly available and released under a Creative Commons CC0 license.

7 Code availability

The code is available in this repository.

8 Author contributions

NR: Methodology, Software, Formal analysis, Visualization, Writing – Original Draft. YQ: Writing – Review & Editing. MS: Writing – Review & Editing. AE: Conceptualization, Methodology, Supervision, Writing – Review & Editing. MvG: Conceptualization, Methodology, Supervision, Writing – Review & Editing.

9 Declaration of competing interests

The authors declare no competing interests.

10 Acknowledgements

This publication is part of the project Dutch Brain Interface Initiative (DBI2) with project number 024.005.022 of the research programme Gravitation which is (partly) financed by the Dutch Research Council (NWO). This project was partly funded by a fellowship supported by the European Laboratory for Learning and Intelligent Systems (ELLIS) Unit Nijmegen and the Radboud University - Maastricht University collaboration fund (Neural Control Program).

References

- Abdul, Z. K., & Al-Talabani, A. K. (2022). Mel frequency cepstral coefficient and its applications: A review. *IEEE Access*, *10*, 122136–122158. <https://doi.org/10.1109/ACCESS.2022.3223444>
- Adolf, D., Weston, S., Baecke, S., Luchtman, M., Bernarding, J., & Kropf, S. (2014). Increasing the reliability of data analysis of functional magnetic resonance imaging by applying a new blockwise permutation method. *Frontiers in Neuroinformatics*, *8*. <https://doi.org/10.3389/fninf.2014.00072>
- Ajith, M., & Calhoun, V. D. (2024). Denoising diffusion probabilistic models for high-fidelity fMRI intrinsic connectivity network data generation. *2024 IEEE EMBS International Conference on Biomedical and Health Informatics (BHI)*, 1–4. <https://doi.org/10.1109/BHI62660.2024.10913576>
- Alowadi, N., Shen, Y., & Tiño, P. (2016). Prototype-based spatio-temporal probabilistic modelling of fMRI data. In E. Merényi, M. Mendenhall, & P. O'Driscoll (Eds.), *Advances in Self-Organizing Maps and Learning Vector Quantization* (pp. 193–203, Vol. 428). Springer. https://doi.org/10.1007/978-3-319-28518-4_17
- Antoniades, A., Yu, Y., Canzano, J., Wang, W., & Smith, S. L. (2024). Neuroformer: Multimodal and multitask generative pretraining for brain data. <https://arxiv.org/abs/2311.00136>
- Arieli, A., Sterkin, A., Grinvald, A., & Aertsen, A. (1996). Dynamics of ongoing activity: Explanation of the large variability in evoked cortical responses. *Science*, *273*(5283), 1868–1871. <https://doi.org/10.1126/science.273.5283.1868>
- Battle, A., Chechik, G., & Koller, D. (2007). Temporal and cross-subject probabilistic models for fMRI prediction tasks. In B. Schölkopf, J. Platt, & T. Hoffman (Eds.), *Advances in Neural Information Processing Systems* (pp. 129–136, Vol. 19). MIT Press. <https://doi.org/10.7551/mitpress/7503.003.0020>
- Bayazi, M. J. D., Ghonia, H., Riachi, R., Aristimunha, B., Khorasani, A., Arefin, M. R., Darabi, A., Dumas, G., & Rish, I. (2024). General-purpose brain foundation models for time-series neuroimaging data. *NeurIPS Workshop on Time Series in the Age of Large Models*. <https://openreview.net/forum?id=HwDQH0r37l>
- Boyle, J., Pinsard, B., Borghesani, V., Paugam, F., DuPre, E., & Bellec, P. (2023). The Courtois Neuro-Mod project: Quality assessment of the initial data release (2020). *2023 Conference on Cognitive Computational Neuroscience*.
- Carè, M., Chiappalone, M., & Cota, V. R. (2024). Personalized strategies of neurostimulation: From static biomarkers to dynamic closed-loop assessment of neural function. *Frontiers in Neuroscience*, *18*. <https://doi.org/10.3389/fnins.2024.1363128>
- Caro, J. O., Fonseca, A. H. d. O., Averill, C., Rizvi, S. A., Rosati, M., Cross, J. L., Mittal, P., Zappala, E., Levine, D., Dhodapkar, R. M., Han, I., Karbasi, A., Abdallah, C. G., & van Dijk, D. (2024).

- BrainLM: A foundation model for brain activity recordings. *bioRxiv*. <https://doi.org/10.1101/2023.09.12.557460>
- Chakravarthy, N., Sabesan, S., Tsakalis, K., & Iasemidis, L. (2009). Controlling epileptic seizures in a neural mass model. *Journal of Combinatorial Optimization*, *17*(1), 98–116. <https://doi.org/10.1007/s10878-008-9182-9>
- Chehab, O., Defossez, A., Loiseau, J.-C., Gramfort, A., & King, J.-R. (2022). Deep recurrent encoder: A scalable end-to-end network to model brain signals. <https://arxiv.org/abs/2103.02339>
- Chen, R. T. Q., Rubanova, Y., Bettencourt, J., & Duvenaud, D. (2019). Neural ordinary differential equations. <https://arxiv.org/abs/1806.07366>
- Corsico, A., Rigamonti, G., Zini, S., Celona, L., & Napoletano, P. (2025). The ISLab solution to the Algonauts challenge 2025: A multimodal deep learning approach to brain response prediction. <https://arxiv.org/abs/2508.06499>
- d’Ascoli, S., Rapin, J., Benchetrit, Y., Banville, H., & King, J.-R. (2025). Tribe: Trimodal brain encoder for whole-brain fMRI response prediction. <https://arxiv.org/abs/2507.22229>
- d’Ascoli, S., Rapin, J., Benchetrit, Y., Brookes, T., Begany, K., Raugel, J., Banville, H., & King, J.-R. (2026). A foundation model of vision, audition, and language for in-silico neuroscience. <https://ai.meta.com/research/publications/a-foundation-model-of-vision-audition-and-language-for-in-silico-neuroscience/>.
- Dehaghani, N. S., & Zarei, M. (2025). Pre-stimulus activities affect subsequent visual processing: Empirical evidence and potential neural mechanisms. *Brain and Behavior*, *15*(2), e3654. <https://doi.org/10.1002/brb3.3654>
- Deshpande, G., LaConte, S., James, G. A., Peltier, S., & Hu, X. (2009). Multivariate Granger causality analysis of fMRI data. *Human Brain Mapping*, *30*(4), 1361–1373. <https://doi.org/10.1002/hbm.20606>
- Devlin, J., Chang, M.-W., Lee, K., & Toutanova, K. (2019, June). BERT: Pre-training of deep bidirectional transformers for language understanding. In J. Burstein, C. Doran, & T. Solorio (Eds.), *Proceedings of the 2019 Conference of the North American Chapter of the Association for Computational Linguistics: Human Language Technologies* (pp. 4171–4186, Vol. 1). Association for Computational Linguistics. <https://doi.org/10.18653/v1/N19-1423>
- Dorin, D., Kiselev, N., Grabovoy, A., & Strijov, V. (2024). Forecasting fMRI images from video sequences: Linear model analysis. *Health Information Science and Systems*, *12*(1), 55. <https://doi.org/10.1007/s13755-024-00315-5>
- Duan, Y., Chaudhry, H. T., Ahrens, M. B., Harvey, C. D., Perich, M. G., Deisseroth, K., & Rajan, K. (2025). POCO: Scalable neural forecasting through population conditioning. <https://arxiv.org/abs/2506.14957>

- Dvornek, N. C., Li, X., Zhuang, J., & Duncan, J. S. (2019). Jointly discriminative and generative recurrent neural networks for learning from fMRI. In H.-I. Suk, M. Liu, P. Yan, & C. Lian (Eds.), *Machine Learning in Medical Imaging* (pp. 382–390, Vol. 11861). https://doi.org/10.1007/978-3-030-32692-0_44
- El-Gazzar, A., & van Gerven, M. (2024). Generative modeling of neural dynamics via latent stochastic differential equations. <https://arxiv.org/abs/2412.12112>
- El-Gazzar, A., & van Gerven, M. (2025a). Probabilistic forecasting via autoregressive flow matching. <https://arxiv.org/abs/2503.10375>
- El-Gazzar, A., & van Gerven, M. (2025b). Universal differential equations as a common modeling language for neuroscience. *Frontiers in Computational Neuroscience*, *19*, 1677930. <https://doi.org/10.3389/fncom.2025.1677930>
- Eren, S., Kucukahmetler, D., & Scherf, N. (2025). Multimodal recurrent ensembles for predicting brain responses to naturalistic movies (Algonauts 2025). <https://arxiv.org/abs/2507.17897>
- Faisal, A. A., Selen, L. P. J., & Wolpert, D. M. (2008). Noise in the nervous system. *Nature Reviews Neuroscience*, *9*, 292–303. <https://doi.org/10.1038/nrn2258>
- Favela, L. H. (2021). The dynamical renaissance in neuroscience. *Synthese*, *199*, 2103–2127. <https://doi.org/10.1007/s11229-020-02874-y>
- Feichtenhofer, C., Fan, H., Malik, J., & He, K. (2019). Slowfast networks for video recognition. *2019 IEEE/CVF International Conference on Computer Vision (ICCV)*, 6201–6210. <https://doi.org/10.1109/ICCV.2019.00630>
- Feng, S., Miao, C., Zhang, Z., & Zhao, P. (2024). Latent diffusion transformer for probabilistic time series forecasting. *Proceedings of the AAAI Conference on Artificial Intelligence*, *38*(11), 11979–11987. <https://doi.org/10.1609/aaai.v38i11.29085>
- Friston, K., Harrison, L., & Penny, W. (2003). Dynamic causal modelling. *NeuroImage*, *19*(4), 1273–1302. [https://doi.org/10.1016/S1053-8119\(03\)00202-7](https://doi.org/10.1016/S1053-8119(03)00202-7)
- Garg, R., Cecchi, G. A., & Rao, A. R. (2011). Full-brain auto-regressive modeling (FARM) using fMRI. *NeuroImage*, *58*(2), 416–441. <https://doi.org/10.1016/j.neuroimage.2011.02.074>
- Gifford, A. T., Bersch, D., St-Laurent, M., Pinsard, B., Boyle, J., Bellec, L., Oliva, A., Roig, G., & Cichy, R. M. (2025). The Algonauts project 2025 challenge: How the human brain makes sense of multimodal movies. <https://arxiv.org/abs/2501.00504>
- Gong, Z., Zhou, M., Dai, Y., Wen, Y., Liu, Y., & Zhen, Z. (2023). A large-scale fMRI dataset for the visual processing of naturalistic scenes. *Scientific Data*, *10*(1), 559. <https://doi.org/10.1038/s41597-023-02471-x>

- Güçlü, U., & van Gerven, M. A. J. (2015). Deep neural networks reveal a gradient in the complexity of neural representations across the ventral stream. *Journal of Neuroscience*, *35*(27), 10005–10014. <https://doi.org/10.1523/JNEUROSCI.5023-14.2015>
- Güçlü, U., & van Gerven, M. A. J. (2017). Modeling the dynamics of human brain activity with recurrent neural networks. *Frontiers in Computational Neuroscience*, *11*, 7. <https://doi.org/10.3389/fncom.2017.00007>
- Harrison, S. J., Woolrich, M. W., Robinson, E. C., Glasser, M. F., Beckmann, C. F., Jenkinson, M., & Smith, S. M. (2015). Large-scale probabilistic functional modes from resting state fMRI. *NeuroImage*, *109*, 217–231. <https://doi.org/10.1016/j.neuroimage.2015.01.013>
- Hu, Y., Wang, X., Ding, Z., Wu, L., Zhang, H., Li, S. Z., Wang, S., Zhang, J., Li, Z., & Chen, T. (2025). FlowTS: Time series generation via rectified flow. <https://arxiv.org/abs/2411.07506>
- Hu, Y., Yujiang, Li, W., & Yuan, Y. (2025). Synthesizing realistic fMRI: A physiological dynamics-driven hierarchical diffusion model for efficient fMRI acquisition. *The Thirteenth International Conference on Learning Representations*. <https://openreview.net/forum?id=zZ6TT254Np>
- Immer, A., Lueckmann, J.-M., Chen, A. B.-Y., Li, P. H., Petkova, M. D., Iyer, N. A., Dev, A., Ihrke, G., Park, W., Petruncio, A., Weigel, A., Korff, W., Engert, F., Lichtman, J. W., Ahrens, M. B., Jain, V., & Januszewski, M. (2025). Forecasting whole-brain neuronal activity from volumetric video. <https://arxiv.org/abs/2503.00073>
- Ito, T., Hearne, L. J., & Cole, M. W. (2020). A cortical hierarchy of localized and distributed processes revealed via dissociation of task activations, connectivity changes, and intrinsic timescales. *NeuroImage*, *221*, 117141. <https://doi.org/10.1016/j.neuroimage.2020.117141>
- Kay, W., Carreira, J., Simonyan, K., Zhang, B., Hillier, C., Vijayanarasimhan, S., Viola, F., Green, T., Back, T., Natsev, P., Suleyman, M., & Zisserman, A. (2017). The kinetics human action video dataset. <https://arxiv.org/abs/1705.06950>
- Khosla, M., Ngo, G. H., Jamison, K., Kuceyeski, A., & Sabuncu, M. R. (2021). Cortical response to naturalistic stimuli is largely predictable with deep neural networks. *Science Advances*, *7*(22), eabe7547. <https://doi.org/10.1126/sciadv.abe7547>
- Kidger, P. (2022). On neural differential equations. <https://arxiv.org/abs/2202.02435>
- Kollovich, M., Ansari, A. F., Bohlke-Schneider, M., Zschiegner, J., Wang, H., & Wang, Y. (2023). Predict, refine, synthesize: Self-guiding diffusion models for probabilistic time series forecasting. <https://arxiv.org/abs/2307.11494>
- Kollovich, M., Lienen, M., Lüdke, D., Schwinn, L., & Gunnemann, S. (2025). Flow matching with Gaussian process priors for probabilistic time series forecasting. <https://arxiv.org/abs/2410.03024>

- Li, J., & Tao, D. (2011). A probabilistic model for discovering high level brain activities from fMRI. In B. Lu, L. Zhang, & J. Kwok (Eds.), *Neural Information Processing. ICONIP 2011* (pp. 329–336, Vol. 7062). Springer. https://doi.org/10.1007/978-3-642-24955-6_40
- Li, W., Wang, T., & Ng, W. W. Y. (2023). Population-based hyperparameter tuning with multitask collaboration. *IEEE Transactions on Neural Networks and Learning Systems*, *34*(9), 5719–5731. <https://doi.org/10.1109/TNNLS.2021.3130896>
- Lipman, Y., Chen, R. T. Q., Ben-Hamu, H., Nickel, M., & Le, M. (2023). Flow matching for generative modeling. <https://arxiv.org/abs/2210.02747>
- Liu, T. T. (2016). Noise contributions to the fMRI signal: An overview. *NeuroImage*, *143*, 141–151. <https://doi.org/10.1016/j.neuroimage.2016.09.008>
- Liu, Z., Qin, Y., van Gerven, M., & Stursberg, O. (2025). Synchronization and control in bistable oscillator networks: Towards epilepsy regulation. *IEEE Control Systems Letters*, *9*, 1514–1519. <https://doi.org/10.1109/LCSYS.2025.3582953>
- Lu, Z., Li, A. J., Ladd, A. E., Matveev, P., Deole, A., Shea-Brown, E., Kutz, J. N., & Steinmetz, N. A. (2025). Benchmarking probabilistic time series forecasting models on neural activity. <https://arxiv.org/abs/2510.18037>
- Lueckmann, J.-M., Immer, A., Chen, A. B.-Y., Li, P. H., Petkova, M. D., Iyer, N. A., Hesselink, L. W., Dev, A., Ihrke, G., Park, W., Petrucio, A., Weigel, A., Korff, W., Engert, F., Lichtman, J. W., Ahrens, M. B., Januszewski, M., & Jain, V. (2025). ZAPBench: A benchmark for whole-brain activity prediction in zebrafish. <https://arxiv.org/abs/2503.02618>
- Meijer, C., & Chen, L. Y. (2024). The rise of diffusion models in time-series forecasting. <https://arxiv.org/abs/2401.03006>
- Millidge, B., Seth, A., & Buckley, C. L. (2022). Predictive coding: A theoretical and experimental review. <https://arxiv.org/abs/2107.12979>
- Murray, J. D., Bernacchia, A., Freedman, D. J., Romo, R., Wallis, J. D., Cai, X., Padoa-Schioppa, C., Pasternak, T., Seo, H., Lee, D., & Wang, X.-J. (2014). A hierarchy of intrinsic timescales across primate cortex. *Nature Neuroscience*, *17*, 1661–1663. <https://doi.org/10.1038/nn.3862>
- Naselaris, T., Kay, K. N., Nishimoto, S., & Gallant, J. L. (2011). Encoding and decoding in fMRI. *NeuroImage*, *56*(2), 400–410. <https://doi.org/10.1016/j.neuroimage.2010.07.073>
- Paugam, F., Pinsard, B., Lajoie, G., & Bellec, P. (2024). A benchmark of individual auto-regressive models in a massive fMRI dataset. *Imaging Neuroscience*, *2*, 1–23. https://doi.org/10.1162/imag_a_00228
- Rasul, K., Seward, C., Schuster, I., & Vollgraf, R. (2021). Autoregressive denoising diffusion models for multivariate probabilistic time series forecasting. In M. Meila & T. Zhang (Eds.), *Proceedings*

- of the 38th International Conference on Machine Learning (pp. 8857–8868, Vol. 139). PMLR. <https://proceedings.mlr.press/v139/rasul21a.html>
- Raut, R. V., Snyder, A. Z., & Raichle, M. E. (2020). Hierarchical dynamics as a macroscopic organizing principle of the human brain. *Proceedings of the National Academy of Sciences*, *117*(34), 20890–20897. <https://doi.org/10.1073/pnas.2003383117>
- Roebroeck, A., Formisano, E., & Goebel, R. (2005). Mapping directed influence over the brain using Granger causality and fMRI. *NeuroImage*, *25*(1), 230–242. <https://doi.org/10.1016/j.neuroimage.2004.11.017>
- Rogers, B. P., Katwal, S. B., Morgan, V. L., Asplund, C. L., & Gore, J. C. (2010). Functional MRI and multivariate autoregressive models. *Magnetic Resonance Imaging*, *28*(8), 1058–1065. <https://doi.org/10.1016/j.mri.2010.03.002>
- Rohlf, C. (2025). Generalization in neural networks: A broad survey. *Neurocomputing*, *611*, 128701. <https://doi.org/10.1016/j.neucom.2024.128701>
- Ruthotto, L., & Haber, E. (2021). An introduction to deep generative modeling. *GAMM-Mitteilungen*, *44*(2), e202100008. <https://doi.org/10.1002/gamm.202100008>
- Safari, M. A., & Mohammadbeigi, M. (2012). Probabilistic graphical models for effective connectivity extraction in the brain using fMRI data. *Studies in Health Technology and Informatics*, *180*, 133–137. <https://doi.org/10.3233/978-1-61499-101-4-133>
- Schad, D. C., Dixit, S., Keck, J., Studenyak, V., Shpilevoi, A., & Bicanski, A. (2025). VIBE: Video-input brain encoder for fMRI response modeling. <https://arxiv.org/abs/2507.17958>
- Schaefer, A., Kong, R., Gordon, E. M., Laumann, T. O., Zuo, X.-N., Holmes, A. J., Eickhoff, S. B., & Yeo, B. T. T. (2017). Local-global parcellation of the human cerebral cortex from intrinsic functional connectivity MRI. *Cerebral Cortex*, *28*(9), 3095–3114. <https://doi.org/10.1093/cercor/bhx179>
- Scholz, R., Bagga, K., Ahrends, C., & Barbano, C. A. (2025). Stacked regression using off-the-shelf, stimulus-tuned and fine-tuned neural networks for predicting fMRI brain responses to movies (Algonauts 2025 report). <https://arxiv.org/abs/2510.06235>
- Schwenzer, M., Ay, M., Bergs, T., & Abel, D. (2021). Review on model predictive control: An engineering perspective. *The International Journal of Advanced Manufacturing Technology*, *117*(5-6), 1327–1349. <https://doi.org/10.1007/s00170-021-07682-3>
- Seth, A. K. (2010). A matlab toolbox for Granger causal connectivity analysis. *Journal of Neuroscience Methods*, *186*(2), 262–273. <https://doi.org/10.1016/j.jneumeth.2009.11.020>
- Simony, E., & Chang, C. (2020). Analysis of stimulus-induced brain dynamics during naturalistic paradigms. *NeuroImage*, *216*, 116461. <https://doi.org/10.1016/j.neuroimage.2019.116461>

- Sobczak, F., He, Y., Sejnowski, T. J., & Yu, X. (2021). Predicting the fMRI signal fluctuation with recurrent neural networks trained on vascular network dynamics. *Cerebral Cortex*, *31*(2), 826–844. <https://doi.org/10.1093/cercor/bhaa260>
- Sonkusare, S., Breakspear, M., & Guo, C. (2019). Naturalistic stimuli in neuroscience: Critically acclaimed. *Trends in Cognitive Sciences*, *23*(8), 699–714. <https://doi.org/10.1016/j.tics.2019.05.004>
- Sun, Y., Cabezas, M., Lee, J., Wang, C., Zhang, W., Calamante, F., & Lv, J. (2024). Predicting human brain states with transformer. <https://arxiv.org/abs/2412.19814>
- Svensen, M., Kruggel, F., & von Cramon, D. Y. (2000). Probabilistic modeling of single-trial fMRI data. *IEEE Transactions on Medical Imaging*, *19*(1), 25–35. <https://doi.org/10.1109/42.832957>
- Tomko, G. J., & Crapper, D. R. (1974). Neuronal variability: Non-stationary responses to identical visual stimuli. *Brain Research*, *79*(3), 405–418. [https://doi.org/10.1016/0006-8993\(74\)90438-7](https://doi.org/10.1016/0006-8993(74)90438-7)
- Wein, S., Schüller, A., Tomé, A. M., Malloni, W. M., Greenlee, M. W., & Lang, E. W. (2022). Forecasting brain activity based on models of spatiotemporal brain dynamics: A comparison of graph neural network architectures. *Network Neuroscience*, *6*(3), 665–701. https://doi.org/10.1162/netn_a_00252
- Xiong, H., Chu, C., Fan, L., Song, M., Zhang, J., Ma, Y., Zheng, R., Zhang, J., Yang, Z., & Jiang, T. (2023). The digital twin brain: A bridge between biological and artificial intelligence. *Intelligent Computing*, *2*, 0055. <https://doi.org/10.34133/icomputing.0055>
- Yamins, D. L. K., & DiCarlo, J. J. (2016). Using goal-driven deep learning models to understand sensory cortex. *Nature Neuroscience*, *19*(3), 356–365. <https://doi.org/10.1038/nn.4244>
- Yeo, B. T. T., Krienen, F. M., Sepulcre, J., Sabuncu, M. R., Lashkari, D., Hollinshead, M., Roffman, J. L., Smoller, J. W., Zöllei, L., Polimeni, J. R., Fischl, B., Liu, H., & Buckner, R. L. (2011). The organization of the human cerebral cortex estimated by intrinsic functional connectivity. *Journal of Neurophysiology*, *106*(3), 1125–1165. <https://doi.org/10.1152/jn.00338.2011>
- Zhang, X., Pu, Y., Kawamura, Y., Loza, A., Bengio, Y., Shung, D. L., & Tong, A. (2025). Trajectory flow matching with applications to clinical time series modeling. <https://arxiv.org/abs/2410.21154>
- Zhang, Y., Kim, J.-H., Brang, D., & Liu, Z. (2021). Naturalistic stimuli: A paradigm for multiscale functional characterization of the human brain. *Current Opinion in Biomedical Engineering*, *19*, 100298. <https://doi.org/10.1016/j.cobme.2021.100298>
- Zhou, F., & Becker, B. (2025). Understanding human brain function in real-world environments. *PLOS Biology*, *23*(6), e3003210. <https://doi.org/10.1371/journal.pbio.3003210>